STUDY OF THE POLARIZED STRUCTURE FUNCTIONS OF THE NEUTRON AT LOW Q^2 USING POLARIZED ^{3}He

Seonho Choi*
Temple University
1900 N. 13th Street
Philadelphia, PA 19122, USA
E-mail: choi@jlab.org

We have measured the electron-^{3}He longitudinal and transverse spin dependent inclusive cross sections $^3\vec{\text{He}}(\vec{e}, e')$, in the resonance region over a range of four-momentum transfer from 0.1 to 0.9 GeV^2. From this measurement, the spin dependent structure functions $g_1(x)$, $g_2(x)$ of ^{3}He have been extracted and various moments of the neutron were evaluated. The integral of $g_1(x)$ shows a smooth continuation from the existing high Q^2 data toward $Q^2 \sim 0$. And that of $g_2(x)$ provided the first significant experimental evidence of the Burkhardt-Cottingham Sum Rule on the neutron in our measured Q^2 region. Spin polarizabilities of the neutron (γ_0 and δ_{LT}) were evaluated and compared with the existing chiral perturbation calculations and MAID model. Higher twist effect on $g_2(x)$ was studied from d_2 moments and finally, color polarizabilities of the neutron were extracted from the combined data of the world and Jefferson Lab. Our new results seem to show small higher twist effects in the neutron with a possibility of quark-hadron duality down to $Q^2 \sim 0.5$ GeV^2.

1. Introduction

One of the important goals in nuclear physics is the understanding of the internal structure of the nucleons. Earlier efforts with the inclusive electron scattering has established Quantum Chromo-Dynamics (QCD) as the fundamental theory describing the nucleons. Subsequent development of polarized beam and target has enabled the study of the *spins* inside the nucleons. One major achievement has been the experimental confirmation of the Bjorken sum rule at high four-momentum transfer(Q^2). Also, a surprising result showed that only about 30% of the proton's spin is carried by the quarks. While earlier measurements were focused at high Q^2 region,

*For JLab E94010 Collaboration

progress is being made for other regions of Q^2. Moreover, most of the previous experiments were done on the proton, which makes the neutron data either scarce or less precise, especially, at low Q^2 region below 1 GeV^2. This region is particularly interesting since non-perturbative characteristics of QCD starts to play. And at very low Q^2 region close to zero, Chiral perturbation theory (χPT) provides necessary guidance for understanding experimental results.

We have measured both spin structure functions (g_1 and g_2) of the neutron for Q^2 values from 0.1 GeV^2 to 0.9 GeV^2 using polarized ^{3}He target. In residual mass W, we have covered up to 2 GeV and a little beyond depending on the values of Q^2. From the measured structure functions, various integrals have been formed and compared with QCD sum rules and the existing theoretical calculations. We were also able to extract higher twist effect from combined data base of our results and previous measurements.

2. Experiment

The two spin structure functions were extracted from the spin-dependent differential cross sections of inclusive electron scattering. An electron beam delivered by Jefferson Lab has been used with average polarization of 70% and current up to 15 μA. For the target, a newly made polarized ^{3}He target has been used as an effective neutron target. This target contains high density (about 10 atm) ^{3}He and a small amount of Rb vapor. The Rb atoms are polarized using optical pumping with circularly polarized laser beam. Then the polarization of the Rb atoms were transfered to ^{3}He nucleus via collision process. With this method, we were able to achieve average ^{3}He polarization of 35%. One important feature of this target is the ability to have polarization direction either parallel or perpendicular with respect to the beam direction.

The scattered electrons were detected by the two essentially identical spectrometers sitting at 15.5° on both sides of the beam. Data were collected at six incident beam energies: 5.508, 4.239, 3.382, 2.581, 1.718 and 0.862 GeV.

The experiment covers a range of Q^2 from 0.03 to 1.1 GeV^2, and from the elastic to the edge of the deep inelastic regime, including the quasi-elastic and the resonance regions. Data were taken for both longitudinal and transverse target polarization orientations so that the two spin structure functions $g_1(x, Q^2)$ and $g_2(x, Q^2)$ can be extracted independently. More

details on the experiment can be found elsewhere[1,2].

3. Data Analysis

The measurement gives the following two cross section differences from which the extraction of the spin structure functions $g_1(x,Q^2)$ and $g_2(x,Q^2)$ is straightforward.

$$\frac{d^2\sigma}{dE'd\Omega}(\downarrow\Uparrow - \uparrow\Uparrow) = \frac{4\alpha^2}{MQ^2}\frac{E'}{\nu E}\left[(E+E'\cos\theta)g_1(x,Q^2) - \frac{Q^2}{\nu}g_2(x,Q^2)\right]$$

$$\frac{d^2\sigma}{dE'd\Omega}(\downarrow\Rightarrow - \uparrow\Rightarrow) = \frac{4\alpha^2\sin\theta}{MQ^2}\frac{E'^2}{E}\frac{1}{\nu^2}\left[\nu g_1(x,Q^2) + 2Eg_2(x,Q^2)\right],$$

where the first arrow ($\downarrow$ or $\uparrow$) shows the polarization direction for the electron beam while the second one ($\Uparrow$ or $\Rightarrow$) is for the target polarization.

Once $g_1(x,Q^2)$ and $g_2(x,Q^2)$ are obtained, various integrals can be considered. The most straightforward comparison can be made with the Gerasimov-Drell-Hearn (GDH) sum rule[3,4], which is valid for the real photon ($Q^2=0$). For non-zero Q^2 values as in our measurement, we can define GDH integral as an extension. In terms of structure functions, the GDH integral can be written as

$$I_{\rm GDH} \equiv \frac{16\pi^2\alpha_{\rm em}}{Q^2}\int\left[g_1(x,Q^2) - \frac{4M^2x^2}{Q^2}g_2(x,Q^2)\right]dx.$$

And at $Q^2=0$, GDH sum rule states

$$I_{\rm GDH}(Q^2=0) = -\frac{2\pi^2\alpha_{\rm em}}{M^2}\kappa^2,$$

where κ is the anomalous magnetic moment of the target.

One of the related integral is the first moment of $g_1(x,Q^2)$ structure function,

$$\Gamma_1(Q^2) = \int g_1(x,Q^2)\,dx.$$

The difference of $\Gamma_1(Q^2)$ between the proton and the neutron at large Q^2 gives the Bjorken sum rule[5,6], which has been verified within 10% level at large Q^2 values.

From $g_2(x,Q^2)$ structure function, there is Burkhardt-Cottingham sum rule[7], which states

$$\Gamma_2(Q^2) = \int g_2(x,Q^2)\,dx = 0 \quad \text{for all } Q^2.$$

Unlike the GDH sum rule or Bjorken sum rule which are valid at two extremes of Q^2 values (0 and ∞), this sum rule is valid for all Q^2 values.

At Q^2 values close to zero, two quantities are of particular interest: generalized spin polarizabilities, γ_0 and δ_{LT} defined as

$$\gamma_0(Q^2) = \frac{16M^2\alpha_{\rm em}}{Q^6}\int_0^{x_0} x^2\left\{g_1(x,Q^2) - \frac{4M^2x^2}{Q^2}g_2(x,Q^2)\right\}\,dx$$
$$\delta_{LT}(Q^2) = \frac{16M^2\alpha_{\rm em}}{Q^6}\int_0^{x_0} x^2\left\{g_1(x,Q^2) + g_2(x,Q^2)\right\}\,dx.$$

Due to the additional x^2 weight, the contribution to the integral from the small x region is very small, which is well suited to the experiment.

One interesting feature of the $g_2(x,Q^2)$ structure function is that it contains twist-3 contributions at leading order. As a result, at large Q^2, the following integral, called d_2 matrix element,

$$d_2(Q^2) = \int x^2\left[2g_1(x,Q^2) + 3g_2(x,Q^2)\right]\,dx$$

gives a measure of higher twist effect on $g_2(x,Q^2)$. This d_2 matrix element is related to color polarizabilities χ_E and χ_B.

At low Q^2, the interpretation in terms of matrix element is no longer appropriate, but $d_2(Q^2)$ integral is now related to generalized spin polarizabilities. So the measurement of $d_2(Q^2)$ integral in the intermediate Q^2 region will describe a transition from quark picture (color polarizabilities) to hadron picture (generalized spin polarizabilities).

4. Results

In Figure 1, our result for the GDH integral[1] shows large change from high Q^2 region to $Q^2 = 0$ where the GDH sum rule dictates the value (-232.5 μb for the neutron). One of the phenomenological prediction from MAID model[8] agrees well for the general trend but underestimates in magnitude. Near $Q^2 = 0$, two calculations from χPT are available.[9,10] One of them has included the contribution from the Δ resonance. Due to the uncertainties on the parameters of Δ resonance, the result is shown as a band. It is quite encouraging that our lowest Q^2 result falls within the band showing compatibility between theory and experiment. As shown in the figure, our lowest Q^2 result is more negative than the GDH sum rule value and suggests a turn over before reaching $Q^2 = 0$ point. The result of a new experiment[11] will provide more details for the region below $Q^2 = 0.1$ GeV^2.

In Figure 2, the integral of $g_1(x,Q^2)^{12}$ has been compared with previous measurements[13,14,15,16,17,18], most of them at high Q^2 region, and theoretical models[8,19,20]. Six open circles at Q^2 between 0.1 and 0.9 GeV^2 are integrals of $g_1(x,Q^2)$ up to $W = 2$ GeV^2 covering mostly resonances. The statistical error is of the size of the symbols and the gray band near the y-axis represents systematic errors. To account for the contribution from the high W region, we have used the parametrization of Bianchi and Thomas[21,22] and the result is shown by the corresponding filled circles. Three model calculations[8,19,20] are available in the measured Q^2 region and the calculation by Burkert and Ioffe agrees well with our data.

The Burkhardt-Cottingham sum rule has been tested in Figure 3 by integrating $g_2(x,Q^2)^{12}$. Filled circles are integrals up to $W = 2$ GeV^2 including mostly resonances. The MAID model prediction agrees reasonably well with our measurement. The upper gray band shows our experimental systematic errors. To test the BC sum rule, we need to include two more contributions: elastic and high W. Elastic contributions are calculated with the neutron form factors parametrized by Mergell *et al.*[23] and is shown by the lower curve. The open circles represent the result including elastic contributions. For high W contributions, our estimate is shown by the lower gray band. Within combined uncertainties, it seems that the BC sum rule holds in our measured Q^2 region. At $Q^2 = 5$ GeV^2, the result from SLAC[24] is also compatible with zero within its error.

Our results for generalized spin polarizabilities[25] show a little surprise. Originally, it has been believed that the theoretical calculations[26,27] from χPT are more reliable for δ_{LT} than γ_0. And it has also been argued that the calculations of δ_{LT} might be valid up to $Q^2 = 0.3$ GeV^2 due to the cancellation of resonance effects. However, as Figures 4 and 5 show, our results for δ_{LT} are completely at odds with the existing calculations while γ_0 for the lowest Q^2 agrees with one of the calculations. For both quantities, MAID model agrees reasonably well with the experimental results.

As Figure 6 shows, our result for $d_2(Q^2)^{12}$ agrees well with the MAID model while all the available χPT calculations overestimate it. At $Q^2 = 5$ GeV^2, SLAC result[24] shows a large positive value but a Lattice QCD calculation predicts a small negative value. The trend toward high Q^2 from our data suggests small positive value at $Q^2 = 5$ GeV^2 and another measurement at $Q^2 = 2$ GeV^2 would be very helpful to resolve the issue.

Finally, using the combined data base, color polarizabilities have been extracted from the fitting. For this analysis, only the data with $Q^2 > 0.5$ GeV^2 have been used. In general, we found higher twist effect quite small.

From the global fitting, we have obtained $\chi_E = 0.033 \pm 0.029$ and $\chi_B = -0.001 \pm 0.016$.

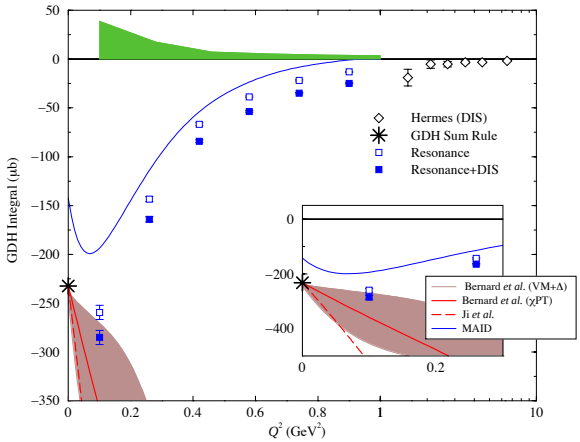

Figure 1. GDH integral as a function of Q^2. To show low Q^2 features more clearly, linear scale has been adopted from $Q^2 = 0$ to 1 GeV^2 and log scale from 1 to 10 GeV^2. Open squares are integrals up to $W = 2$ GeV, while filled squares include contributions up to $W^2 = 1000$ GeV^2 using the parametrization. Experimental errors are shown as grey band above the zero y-axis. Solid curve is from MAID model which shows general feature of our results but underestimates the absolute values. Two curves and grey band are χPT calculations from two different groups.

5. Conclusions

We have measured spin-dependent cross sections for $^3\vec{\mathrm{He}}(e,e')$ and extracted spin dependent structure functions $g_1(x,Q^2)$ and $g_2(x,Q^2)$ at Q^2 range from 0.1 to 0.9 GeV^2. From the two structure functions, various QCD integrals have been evaluated for the neutron for the first time at the intermediate Q^2 range ($0.1 \leq Q^2 \leq 0.9$). The GDH integral shows dramatic change from high Q^2 region toward GDH sum rule at $Q^2 = 0$. Actually, our lowest Q^2 point overshoots the GDH sum rule value and the result of another experiment[11] will provide more detail near $Q^2 = 0$ region. The integral of $g_1(x,Q^2)$, $\Gamma_1(Q^2)$ shows smooth variation from high Q^2 region and a few phenomenological model predicts right trend and magnitude. The integral of $g_2(x,Q^2)$ shows that the Burkhardt-Cottingham sum rule holds within experimental errors in the measured Q^2 region. The result for the generalized spin polarizabilities is quite surprising. δ_{LT} is at odds with

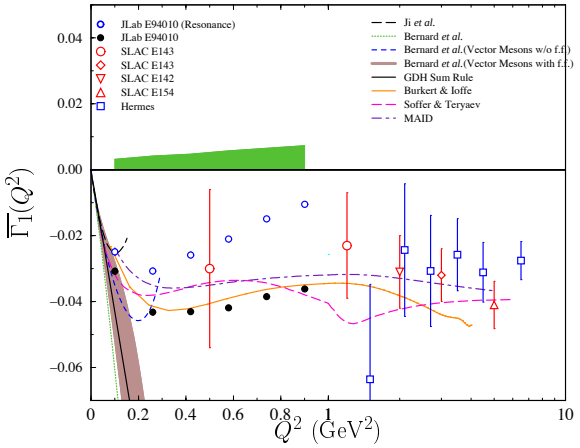

Figure 2. The integral of $g_1(x, Q^2)$ structure function with previous data mostly at large Q^2. Filled circles are our result including estimated contributions from non-measured small x region. Grey band above y-axis shows experimental uncertainties. Various phenomenological models agree reasonably well for both trend and magnitude. Near $Q^2 = 0$, several calculations from χPT are shown.

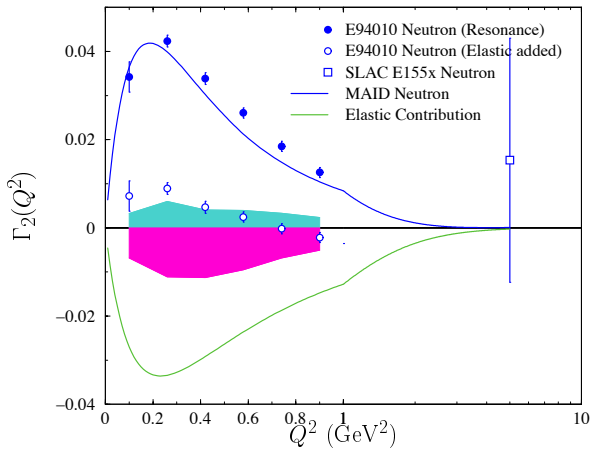

Figure 3. The integral of $g_2(x, Q^2)$ structure function for the Burkhardt-Cottingham sum rule. Open circles are integral over the resonance. To compare with the BC sum rule, the elastic contribution (lower grey curve) has been added to produce open circles. Positive grey band around the y-axis shows experimental uncertainties while negative grey band shows an estimate of contributions from non-measured small x region. At $Q^2 = 5$ GeV^2, SLAC results shows the satisfaction of the BC sum rule within its error.

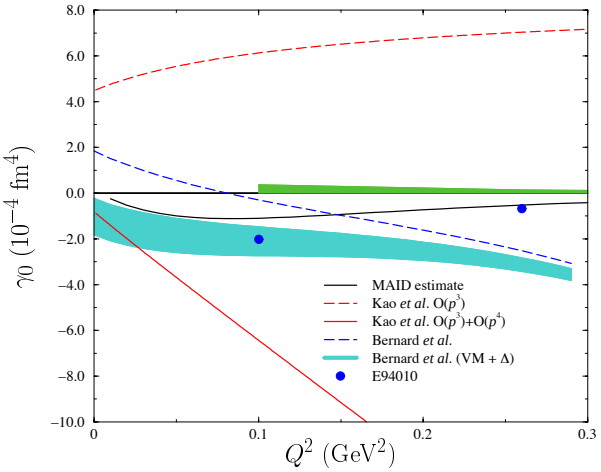

Figure 4. Generalized spin polarizability γ_0. Filled circles are from our measurement. Curves and band are from two different χPT calculations. The band is due to uncertainties on the Δ resonance included in the calculation. Grey band on top of the y-axis shows experimental uncertainties.

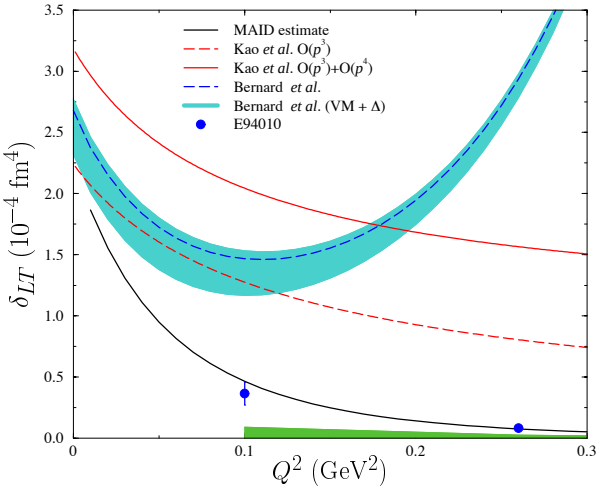

Figure 5. Generalized spin polarizability δ_{LT}. Filled circles are from our measurement. Curves and band are from two different χPT calculations. The band is due to uncertainties on the Δ resonance included in the calculation. Grey band on top of the y-axis shows experimental uncertainties. Except the phenomenological MAID calculation, none of the calculations agree with the experimental result.

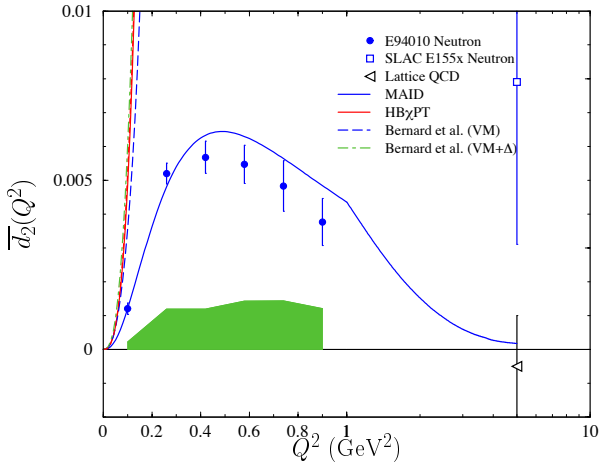

Figure 6. $d_2(Q^2)$ integral. Filled circles are from our measurement. MAID model is in good agreement both in trend and magnitude. At $Q^2 = 5$ GeV^2, SLAC result shows positive d_2 while Lattice QCD calculation predicts small negative value. The general trend from our data predicts small positive value at the same Q^2.

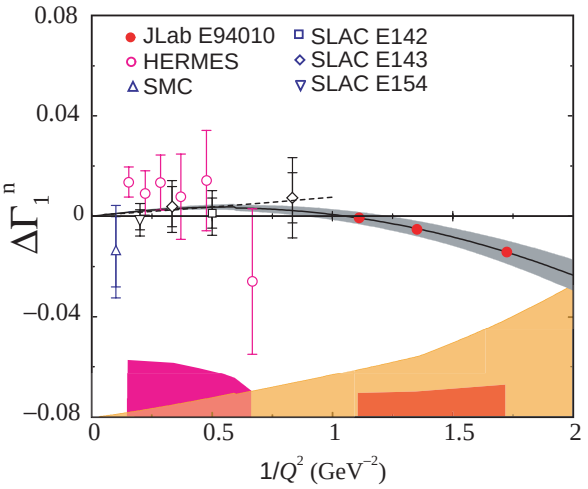

Figure 7. Fitting result of the available world data. The two separate grey bands represent systematic errors for both our measurement and HERMES result. Third band shows overall systematic error including the contribution from α_S. the band near the data point shows the fitting error.

available theoretical calculations, which are believed to be reliable at low Q^2 values. On the other hand, γ_0 shows an agreement at the lowest Q^2

values with one of the calculations.

Combining our results with previous measurements, an attempt has been made to extract color polarizabilities, χ_E and χ_B. Global fitting of all the available data gives quite small values for both color polarizabilities. Such small values suggests small higher twist effect down to $Q^2 \simeq 0.5$ GeV^2 and indirectly confirms quark-hadron duality of spin structure functions.

New experiment[11] has been performed to explore smaller Q^2 region down to 0.02 GeV^2 and its results will reveal even more interesting features.

References

1. M. Amarian *et al.,* Phys. Rev. Lett. **89**, 242301 (2002).
2. http://www.jlab.org/e94010.
3. S. B. Gerasimov, Sov. J. Nucl. Phys. **2**, 430 (1966).
4. S. D. Drell and A. C. Hearn, Phys. Rev. Lett. **16**, 908 (1966).
5. J. D. Bjorken, Phys. Rev. **148**, 1467 (1966).
6. J. D. Bjorken, Phys. Rev. D **1**, 1376 (1970).
7. Hugh Burkhardt and W. N. Cottingham, Annals of Physics **56**, 453 (1970).
8. D. Drechsel, S. Kamalov and L. Tiator, Phys. Rev. D **63**, 114010 (2001).
9. X. Ji and J. Osborne, J. Phys. G **27**, 127 (2001).
10. V. Bernard, T. Hemmert and Ulf-G. Meissner, Phys. Lett. **B 545**, 105 (2002).
11. J.-P. Chen, A. Deur and F. Garibaldi, JLab proposal E97110, *The GDH Sum Rule and the Spin Structure of* ^{3}*He and the Neutron using Nearly Real Photons.*
12. M. Amarian *et al.,* Phys. Rev. Lett. **92**, 022301 (2004).
13. P. L. Anthony *et al.*, Phys. Rev. Lett. **71**, 959 (1993).
14. P. L. Anthony *et al.*, Phys. Rev. D **54**, 6620 (1996).
15. K. Abe *at al.*, Phys. Lett. **B 364**, 61 (1995).
16. K. Abe *at al.*, Phys. Rev. D **58**, 112003 (1998).
17. K. Abe *at al.*, Phys. Rev. Lett. **79**, 26 (1997).
18. A. Airapetian *et al.*, Eur. Phys. J. **C 26**, 527 (2003).
19. J. Soffer and O. V. Teryaev, Phys. Lett. **B 545**, 323 (2002).
20. V. D. Burkert and B. L. Ioffe, Phys. Lett. **B 296**, 223 (1992).
21. N. Bianchi and E. Thomas, Phys. Lett. **B 450**, 439 (1999).
22. N. Bianchi and E. Thomas, Nucl. Phys. B, Proc. Suppl. **82**, 256 (2000).
23. P. Mergell, Ulf-G. Meissner and D. Drechsel, Nucl. Phys. **A596**, 367 (1996).
24. P. L. Anthony *et al.*, Phys. Lett. **B 553**, 18 (2003).
25. M. Amarian *et al.,* Phys. Rev. Lett. **93**, 152301 (2004).
26. C. W. Kao, T. Spitzenberg and M. Vanderhaeghen, Phys. Rev. D **67**, 016001 (2003).
27. V. Bernard, T. Hemmert and Ulf-G. Meissner, Phys. Rev. D **67**, 076008 (2003).